JOURNAL OF AIRCRAFT
Vol. 43, No. 4, July–August 2006

Hysteresis and Broad Flow Features on a Swept Wing at High Lift

L. Venkatakrishnan,* S. Sundaram,† and P. R. Viswanath‡
National Aerospace Laboratories, Bangalore 560 017, India

Experiments have been performed at low speeds documenting certain broad aspects of hysteresis on a mildly swept wing under high-lift conditions. Aerodynamic load measurements were carried out at two values of incidence, 10.5 and 15.5 deg, and flap deflections of 20 and 30 deg, essentially under quasi-steady conditions. Two-dimensional particle image velocimetry (PIV) was utilized to measure the mean velocity vector field in the rear part of the wing and flap. These velocity measurements have revealed the complex nature of separated flows on the wing and flap. Also, in general, the slot flow angle determined by geometric considerations is very different from those actually inferred from PIV measurements.

Nomenclature

A_w = wing area, 0.3 m^2
C_L = lift coefficient, [lift force/(freestream dynamic head × wing area)]
C_D = drag coefficient, [drag force/(freestream dynamic head × wing area)]
q_∞ = freestream dynamic head
$\boldsymbol{U}$ = local velocity, m/s
$\boldsymbol{U}_\infty$ = freestream velocity, m/s
α = angle of incidence, deg
δ_f = flap deflection, deg

Introduction

THE last two decades have seen considerable research activity on the subject of high-lift flows relevant to transport aircraft. The flowfield with multi-elements deployed can be quite complex,[1–4] involving three dimensionality, transition by different flow mechanisms, confluent viscous layers, and boundary-layer separation. The major difficulty in predicting these flows at high lift is, of course, coupled with the inherent difficulty in accurately modeling turbulence in such flow situations. It has been suggested[2] that increased attention be paid to understanding and modeling of the fundamental fluid mechanics related to high-lift flows in the future.

Reliable experimental data at high lift involving both mean and turbulence quantities are essential to improve flow modeling. Several experimental studies[5–9] on two-dimensional high-lift configurations have been reported, and hot-wire anemometry has been utilized to obtain mean and turbulence data. There have also been some attempts[10] to measure the flowfield using laser velocimetry. The use of two-dimensional particle image velocimetry (PIV) is relatively recent,[11] but very attractive from the point of view of documenting the velocity field in a given plane including flow reversal.

In the context of high-lift flows, unsteady effects have received very little attention. Although hysteresis effects are well known[12,13] on low Reynolds number airfoils, it is only in the recent past that some information on hysteresis effects on two-dimensional airfoils with a flap at relatively high Reynolds numbers has been reported. Biber and Zumwalt[14] studied hysteresis effects on a 13% thick general aviation wing or GAW-2 airfoil with 25% slotted flap at a chord Reynolds number of 2.2×10^6. The boundary layer on the airfoil was tripped on both the upper and lower surfaces. The test matrix included flap nested as well as deflected cases of 30 and 40 deg with optimum and narrow gaps. The measurements made included the aerodynamics loads on the airfoil–flap system using a pyramidal-type balance and static pressures along the midspan of the airfoil and flap. The balance measurements were in a pitch and pause made over an incidence α range of -8 to 22 deg; at each value of α, force/moment data samples were taken 0.2 s. apart for a total period of 2 s. Essentially, the load measurements were made in a quasi-steady sense. They observed varying degrees of hysteresis as dependent on flap deflection and the gap ratio: For example, hysteresis effects were more severe for the flap deflection of 40 deg, and narrowing the gap reduced the size of the hysteresis loop. They suggested[14] that the hysteresis loop was primarily a result of the change of flow pattern about the flap rather than the main airfoil and, further, the slot flow angle and gap width were relevant factors in determining the level of hysteresis.

Recently Landman and Britcher[15] reported results of lift hysteresis on a modern three-element airfoil under high-lift conditions. The chord Reynolds number was 1×10^6 and lift characteristics were obtained by integration of measured surface pressure data. Hysteresis was observed as a function of flap position for fixed model incidence and freestream conditions. It was suggested[15] that the occurrence of such a hysteresis phenomenon could present a serious challenge to flap optimization studies.

Several issues related to the occurrence of hysteresis under high-lift conditions are of significant engineering interest: What are the conditions leading to hysteresis and what is the flow topology associated with it on two-dimensional airfoil–flap configurations? Will hysteresis occur at higher Reynolds numbers typical of flight conditions? What are the features of hysteresis on swept wings (of relevance to transport aircraft), if it occurs? Significant experimental effort is needed in the future to be able to answer some of these questions.

In this paper, we report results associated with hysteresis observed on a mildly swept wing with a slotted flap under high-lift conditions. In addition to measurements of aerodynamic loads employing a floor (or half-model) balance, the separated flow in the rear part of the wing section and flap was documented using two-dimensional PIV for certain selected test cases. The balance measurements were made in a quasi-steady sense, as in Ref. 14. The velocity field obtained using PIV for the different cases reveal complex flow features associated with hysteresis.

Received 1 May 2005; revision received 27 September 2005; accepted for publication 27 September 2005.

*Scientist, Experimental Aerodynamics Division. Member AIAA.
†Professor, Department of Mechanical Engineering; currenttly Professor, Department of Mechanical Engineering, Sir M Visveswaraya Institute of Technology, Bangalore 562 157, India.
‡Head, Experimental Aerodynamics Division. Associate Fellow AIAA.

Experiments

Wing Model

The experiments were carried out on a half-wing model to study the effects of gap, overlap, and flap deflection angle on hysteresis under high-lift conditions. The geometric details of the mildly swept wing model are presented in Fig. 1. The wing chosen was based on the current interest at the National Aerospace Laboratories (NAL) on small transport aircraft, and besides, it was thought that hysteresis effects on a mildly swept wing would be broadly similar to those on two-dimensional airfoil–flap configurations.

The cross section of the wing section was a 13.6% thick GAW-2 airfoil and carried a 25% chord slotted flap in the inboard part of the wing (Fig. 2).

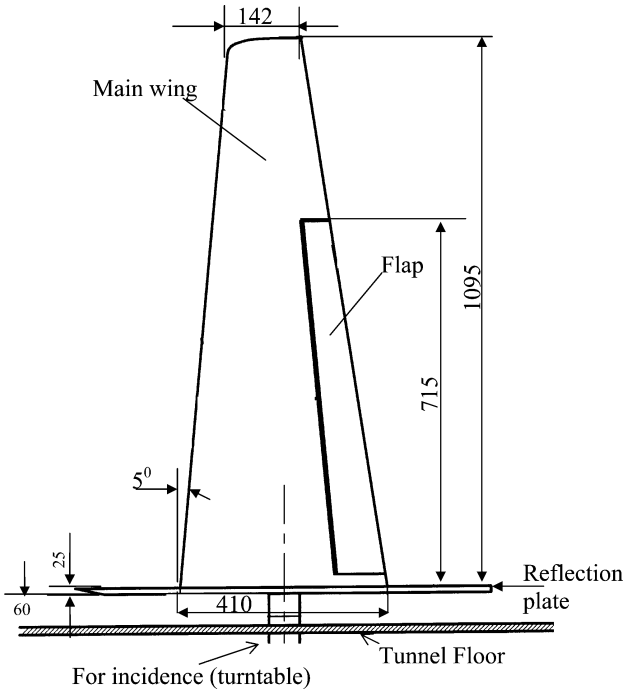

Fig. 1 Geometric details of wing model (all dimensions in millimeters).

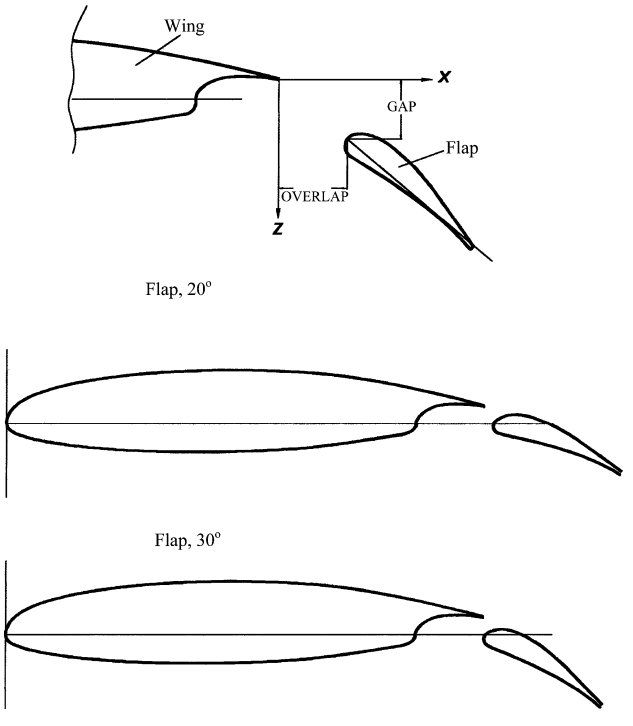

Fig. 2 Wing geometry at different flap settings.

The flap was attached to the main wing through end linkages, which allowed flap setting at any desired overlap and gap. The flap could be fixed at any desired location (of any desired gap and overlap) using flap brackets. The gap and overlap chosen were those determined as optimum for this configuration during an earlier study on the same wing. The wing boundary layers on the upper and lower surfaces were tripped at a distance of 10% chord from the leading edge using 50 grade sand paper of 10 mm width. This wing model was tested in two low-speed wind-tunnel facilities which are described next.

Wind-Tunnel Facilities

The wing aerodynamic load measurements were carried out in the 4.25×2.75 m open-circuit wind tunnel at the Indian Institute of Science, Bangalore, India. The maximum speed attainable was 50 m/s, and the freestream turbulence was 0.13% at this speed. The wing model was mounted vertically in the tunnel on top of the floor half-model balance, and a reflection plate was used at the wing root section to minimize interference from the tunnel wall boundary layer (Fig. 1). The wing incidence could be varied remotely in a pitch–pause mode from -6 to $+20$ deg. Limited tuft flow visualization studies were carried to get a broad idea of flow separation on the wing.

The 1.5×1.5 m low-speed wind tunnel (at NAL, Bangalore, India) was utilized for two-dimensional PIV measurements. This wind tunnel, being of moderate size, could be well exploited for PIV measurements, which were considered very important in this study. The freestream velocity in this tunnel can be varied in the range of 10–55, m/s and freestream turbulence level is within 0.12% in that speed range. A reflection plate at the wing root section, very similar to that utilized for balance loads, was employed for the PIV measurements in this tunnel as well.

The solid model blockage for the load measurements (in the 4.25×2.75 m wind tunnel) and the PIV measurements in the two tunnels were 1% and 4.5%, respectively, for the maximum incidence and flap conditions chosen here; we expect wall interference effects even for PIV measurements to be small.

Instrumentation and Measurements Made

The half-model loads were measured using an accurate six-component floor balance having the following load capacities: normal force = 700 kgs, axial force = 25 kgs, side force = 250 kgs, pitching moment = 50 kg · m, rolling moment = 200 kg · m and yawing moment = 70 kg · m. With the tunnel speed set at 40 m/s, the model incidence was varied in the range from -6 to $+20$ deg (at 2-deg intervals) in the pitch and pause mode. On reaching α_{max} of 20 deg, the model incidence was lowered in the pitch–pause mode back to -6 deg. At each α, the balance data were acquired at a rate of 3000 samples per second simultaneously for all balance elements for a period of 1.8 s preceded by a dwell time of 0.2 s. Essentially data were acquired with the model having a fixed incidence for 2 s in a manner very similar to the procedure used by Biber and Zumwalt[14] in their two-dimensional airfoil–flap hysteresis study. This procedure was adopted essentially to document hysteresis effects under quasi-steady conditions and to be able to observe similarities (or otherwise) in the broad features of hysteresis in relation to those seen on a two-dimensional airfoil–flap configuration.[14] The digital data acquired was processed to yield forces and moments using a Pentium-based personal computer.

Two-component PIV measurements were carried out in the NAL 1.5×1.5 m wind tunnel, and the experimental arrangement is shown in Fig. 3. The flowfield with seed particles was illuminated by a double-pulsed, frequency-doubled dual Nd: YAG, PIV 400 laser. The optimum performance of the laser is at 15 Hz. It was, therefore, possible to obtain 15 pairs of images per second using this laser. The laser was mounted on a platform at the height of the tunnel floor and not in physical contact with the tunnel (to avoid possible vibrations to the system). The beam steering was achieved by a pair of Nd-YAG mirrors mounted on the base and carrier of the vertical axis of a two-dimensional traverse. With this arrangement, the beam could be positioned at any point in a two-dimensional plane perpendicular to

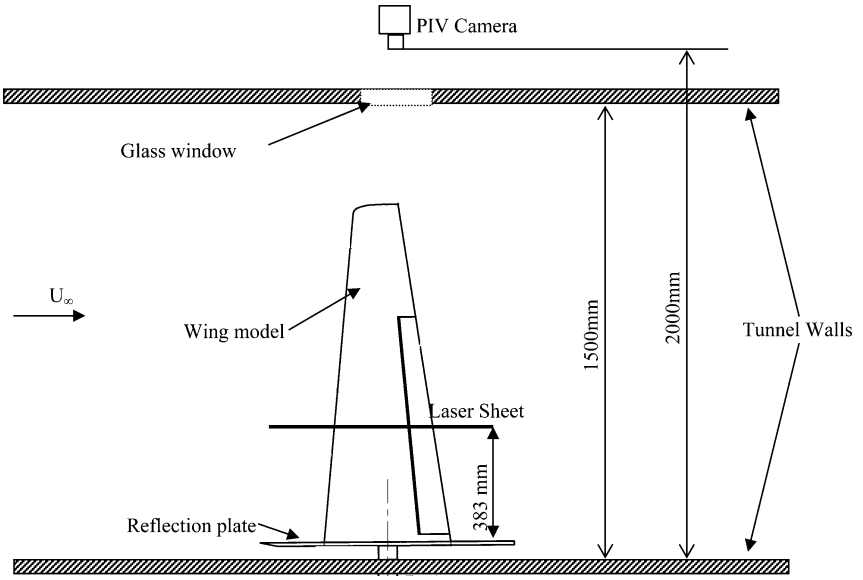

Fig. 3 Schematic of experimental setup.

the flow. The beam then passed through the beam-forming optics and was spread as a thin (0.8-mm) sheet of light with nearly flat intensity profile in the measurement plane using a combination of negative and positive spherical lenses and a cylindrical lens. The sheet entered the tunnel 0.5 m downstream of the test section through a window in the tunnel wall. This ensured that the sheet did not vibrate during tunnel runs and yield spurious turbulence data.

The flow was imaged using a Kodak ES 1.4 progressive scan digital charge-coupled device (CCD) camera having a sensor resolution of 1008 (horizontal) × 1018 (vertical) pixels. The camera was mounted on an overhanging arm from a vertical post, which was firmly fixed on the laboratory floor. A Nikon 50-mm normal lens was used as the imaging optics for the CCD. This provided a near flat focus of the viewing area of 140 mm square at a distance of 1 m. The CCD camera operated in synchronization with the laser pulsing. The synchronization of the laser pulsing with camera and the grabbing of the images are carried out using an IDT-1000 controller from IDT Systems.

The cross-correlation CCD is capable of recording two successive images separated in time as low as 1 μs and stores them in the local buffers, which are then transferred to the personal computer memory using a NI-IMAQ image grabbing card. The main memory of the personal computer restricts the number of pairs of images that can be acquired per batch. Each pair of images requires 2-MB space, and in the present setup with the personal computer RAM of 1 GB, it is possible to acquire 500 pairs per batch.

The PIV image acquisition and processing was carried out by IDT ProVISION® software. This software also allows usage of an unconstrained mesh for processing, which was used to configure a mesh for each case that would allow the best possible resolution.

Application of PIV in a relatively large open-circuit tunnel such as the present 1.5-m low-speed wind tunnel posed many problems. Preliminary studies were carried out to address the problems of uniformly seeding such a complex separated flow and obtaining the mean flowfield on a finite wing. The uniformity and quantity of seeding was seen to have a direct relation to the quality of the data. Two fogging machines (Antari Z- Series fog machine, 1500 W and 40,000 ft^3/min or 18 cubic meter/second using Antari standard fog fluid gallon) were used in this experiment to introduce seeding into the flow, especially at the plane of interest. Earlier phase Doppler particle analyzer measurements on a fogger of identical design showed the particle size distribution to be Gaussian with a mean size of 5 μm (Ref. 16). The maximum particle size encountered was 10 μm. The size range is satisfactory for following the flow without lag for the present test conditions. Uniformity in seeding is crucial for capturing good pictures of a flow. Too much seeding causes light saturation on the CCD and should be avoided. Several trials proved that the seeding could not be concentrated only to the plane of interest, but had to be made uniform over the entire tunnel cross section.

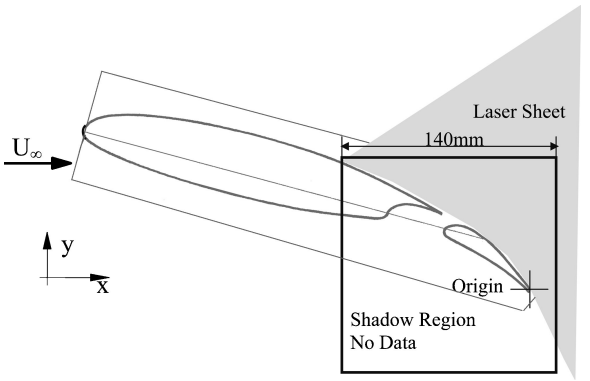

Fig. 4 Flow mapping geometry.

The velocity field was measured in a two-dimensional plane parallel to the freestream (Fig. 3). Because the wing was mildly swept, the dominant flow was expected to be generally along the freestream with some small three-dimensional effects. The velocity field in a plane parallel to the freestream direction must therefore provide an excellent representation of the mildly three-dimensional flow around the wing.

The plane visualized was in the midflap region, 383 mm from the wing root (Fig. 3). The image area and interrogation cell size were chosen after a preliminary study examining the accuracy of PIV velocity data with a hot wire in the near wake of this wing for the nested configuration. After this exercise, the following parameters were chosen. The area imaged was 140 × 140 mm, that is, each pixel was 0.14 mm in physical space. The images were separated by a time delay of 12 μs. The interrogation cell size was chosen as 20 × 20 pixels, and this resulted in a physical resolution of 2.8 mm.

The laser sheet was incident from the wing upper side; the flow over the bottom of the wing could not be visualized (Fig. 4). The flow mapped by PIV was restricted to covering the rear part of the wing and the flap section, in a region 140 × 140 mm extending 10 mm downstream of the flap trailing edge, which is also schematically shown in Fig. 4. The trailing edge of the flap was fixed as origin for presenting the results. All of the PIV mean velocity data were computed from 2000 pairs of images, and as a result the data are considered virtually free of statistical errors.

Flow Visualization

Tuft flow visualization was undertaken to provide qualitative information on the nature of the flow on the wing and flap with increasing and decreasing angle of attack. Photographs were taken under quasi-steady conditions at selected values of α.

Test Matrix

All of the tests were made at a freestream velocity of 40 m/s, and the Reynolds number based on root chord was 1.2×10^6. The balance data were acquired in the incidence range from -6 to $+20$ deg (at 2-deg intervals) for flap deflections δ_f of 10, 20, 30, and 40 deg. In this paper, however, we present data only at $\delta_f = 20$ and 30 deg essentially to bring out certain interesting features of the hysteresis phenomena observed. The two-dimensional PIV measurements were, therefore, restricted to the flap angles of 20 and 30 deg; in addition acquiring good PIV data turned out to be quite time consuming. At each of the two flap angles, two values of model incidence of 10.5 and 15.5 deg were covered. These α values were selected based on the lift hysteresis curve (to be discussed in the next section). Also note that the PIV measurements were made under steady conditions at the selected valves of δ_f and α (unlike balance data described earlier) because conditionally sampled PIV measurements, more appropriate with hysteresis effects, would be an extremely difficult task. It was recognized that knowledge of the velocity field, even under steady conditions, would be meaningful for a first cut understanding of the flow topology associated with hysteresis.

Measurement Uncertainties

The floor balance used for the wing loads was calibrated before the test series, and the accuracy of the balance system was found to be better than 0.5% of the rating of the balance elements. When repeat runs are taken into account, the estimates of uncertainties in C_L and C_D are

$$\Delta C_L < \pm 0.02 C_L (20-1), \qquad \Delta C_D < \pm 0.02 C_D (20-1)$$

For the fog fluid utilized and kind of atomizer used, the average particle diameter is expected in the range of 5–10 μm (Ref. 16), which is generally considered adequate for low-speed PIV measurements.To quantify any effects due to nonuniform seeding and particle-size effects, comparisons of mean velocity from PIV were carried out against hot-wire measurements in the near wake for the flap nested condition. With 2000 pairs of images utilized for the determination of the mean velocity field, we expect the statistical errors due to averaging to be very small. In essence, the uncertainty in the velocity vector $\boldsymbol{U}$ is expected to be generally less than 1 m/s. Despite the surface having a smooth finish, due to the reflection of the laser light toward the camera, it was not possible to obtain good PIV data closer than 2 mm from the surface.

Results and Discussion

The force/moment measurements using the balance were made for several flap deflections δ_f, but we present here results only at $\delta_f = 20$ and 30 deg to bring out certain essential features of hysteresis. The force data, normalized by the freestream dynamic pressure and wing area (flap in nested condition), are presented here.

Lift and Drag Characteristics

The lift and drag characteristics for $\delta_f = 20$ and 30 deg are presented in Figs. 5 and 6, respectively, where data corresponding to increasing and decreasing α are indicated by arrows. Also shown are the incidence angles of 10.5 and 15.5 deg chosen for PIV investigations. At $\delta_f = 20$ deg, the hysteresis loop is relatively small with a loss in lift ΔC_L of about 0.30 (Fig. 5). The onset of hysteresis occurs around $\alpha = 14$ deg and reattachment around the same α. (In hysteresis literature, the terminology reattachment is sometimes used to indicate the end or close of hysteresis loop while α is decreased.) At the higher flap deflection angle of 30 deg, the lift and drag characteristics reveal a complex double loop over a considerable α range, with the final reattachment occurring at $\alpha = -4$ deg (Fig. 6). It is obvious that the separated flow features on the wing–flap combination are indeed significantly different for increasing and decreasing α at this flap deflection. The force/moment data, measured during repeat tunnel runs, were in very good agreement, suggesting that the flow phenomena associated with hysteresis at each α are relatively steady as far as time-averaged or mean properties are concerned.

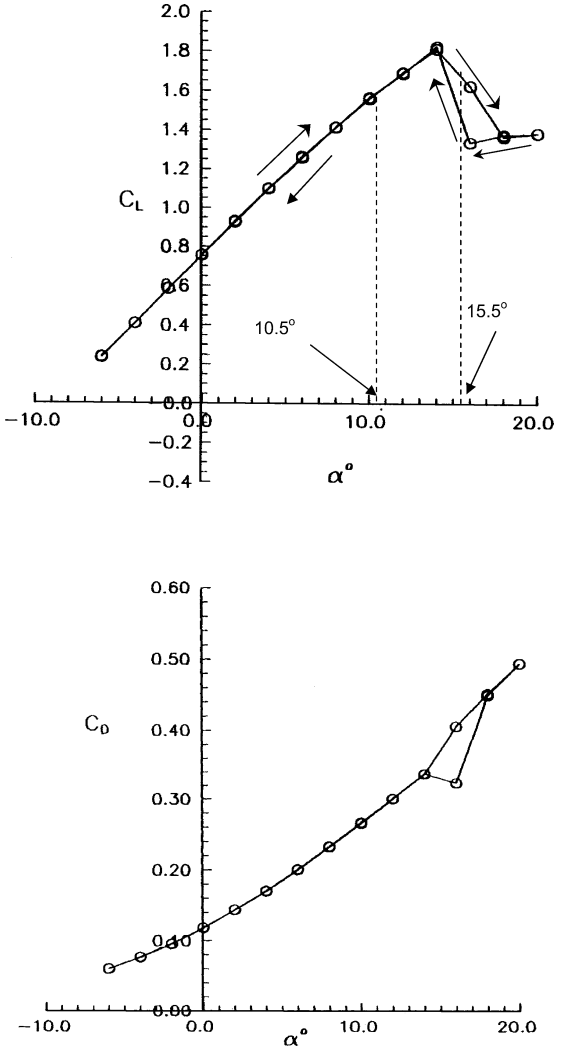

Fig. 5 Lift and drag characteristics for flap deflection $\delta_f = 20$ deg.

Tuft Flow Visualization

To bring out certain broad features of separated flows on the wing–flap combination, tuft-flow photographs were taken at selected α (with α increasing) under quasi-steady conditions (in a manner similar to those of balance measurements). Photographs at $\alpha = 6$, 12, and 18 deg for $\delta_f = 20$ and 30 deg are shown in Figs. 7 and 8, respectively. For flap angle of 20 deg, the flow is attached everywhere at $\alpha = 6$ deg, and a progressive increase in the separated flow on the flap and wing may be observed at $\alpha = 12$ and 18 deg. At $\delta_f = 30$ deg, the wing flow is attached, whereas the flap flow is separated even at $\alpha = 6$ deg; a larger degree of separated flow is seen $\alpha = 12$ and 18 deg (compared to $\delta_f = 20$ deg) consistent with increased adverse pressure gradients expected with higher flap deflection. These flow visualization studies indicate (in a gross sense) existence of separated flows on the wing, as well as on the flap at higher α (>12 deg).

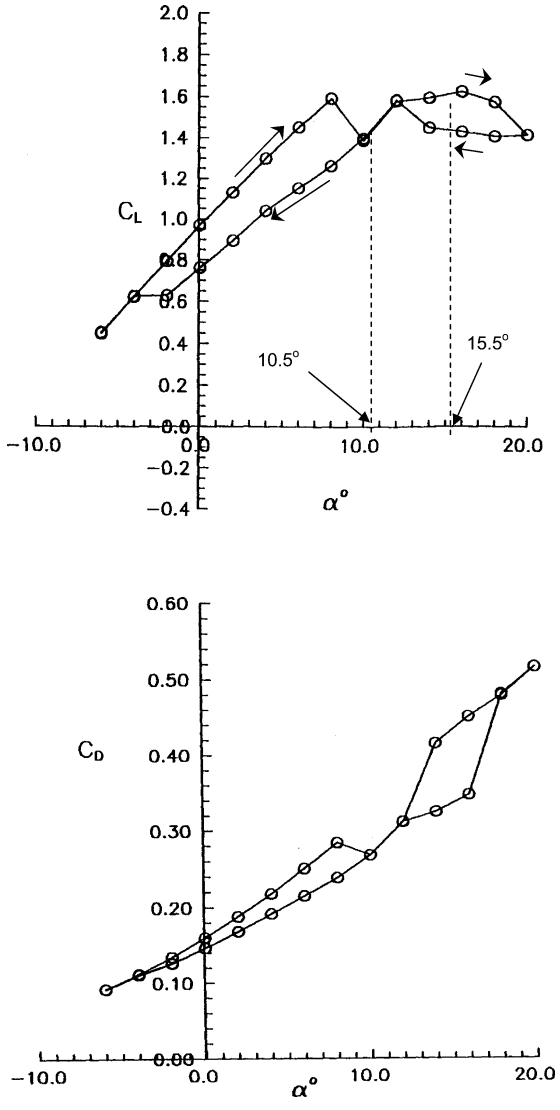

Fig. 6 Lift and drag characteristics for flap deflection $\delta_f = 30$ deg.

Mean Velocity Field Measured by PIV

Here we present the PIV mean velocity field obtained in the rear part of the wing and on the flap for two values of incidence of 10.5 and 15.5 deg and flap deflection of 20 and 30 deg. The velocity field is presented in physical units (meter per second) essentially to observe the relative magnitudes of the velocities including reverse flow in the different regions.

Mean Velocity Field for $\delta_f = 20$ Degrees

The mean velocity vector maps at $\alpha = 10.5$ deg and $\alpha = 15.5$ deg for flap deflection of $\delta_f = 20$ are shown in Figs. 9 and 10, respectively. The reference vector scale is chosen as the freestream velocity (40 m/s). The vectors are two-color coded to the sign of the velocity along the freestream direction, thus enabling easy recognition of separated zones. As may be observed, there are insufficient data close to the surface, due to the reasons discussed earlier; in particular, in the reversed flow ahead of the main wing trailing edge (Fig. 10), the correlation resulted in unreliable data up to $y = 2$ mm from the surface and they have been deleted in Fig. 10.

With reference to Figs. 9 and 10, it is clear that with increase in incidence, there is a deceleration of velocity field on the wing and the flap as a result of increased streamwise adverse pressure gradient. In particular, at $\alpha = 15.5$ deg, there is a weak separation just ahead of the trailing edge of the main wing, and flap flow, beyond about 50% flap chord, is separated as well.

These observations are broadly consistent with the flow visualizations shown in Fig. 7. The wakelike structure of the shear flow downstream of the trailing edge of the main wing may be clearly seen at both values of α. At both of the angles of incidence, the slot flow may be observed to be nearly parallel to the local flap surface; the local velocity in the flap leading edge zone is relatively lower at $\alpha = 15.5$ deg because of higher streamwise pressure gradient. The flap flow is largely influenced by the slot flow and behaves like a wing at an angle of 20 deg to the freestream.

Mean Velocity Field for $\delta_f = 30$ Degrees

The mean velocity field for $\delta_f = 30$ deg, presented in Figs. 11 and 12, respectively, show dramatically different features compared to those in Figs. 9 and 10.

At $\alpha = 10.5$ deg, the flow ahead of the main wing trailing edge shows significant deceleration compared to the results at

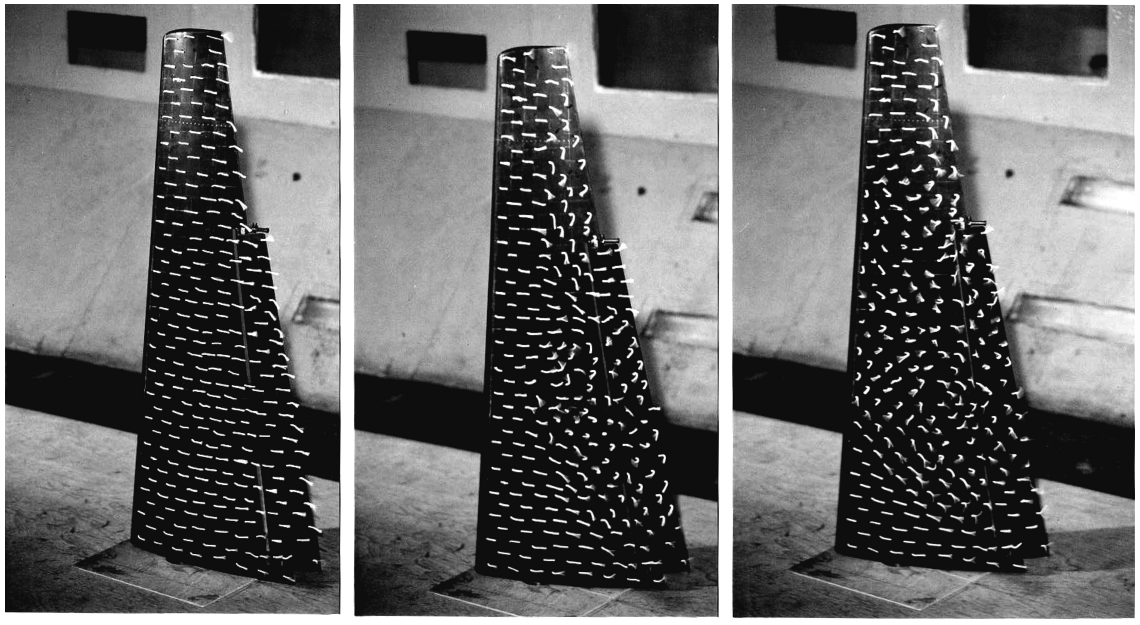

a) $\alpha = 6$ deg **b) $\alpha = 12$ deg** **c) $\alpha = 18$ deg**

Fig. 7 Wing flow patterns using tufts at $\delta_f = 20$ deg.

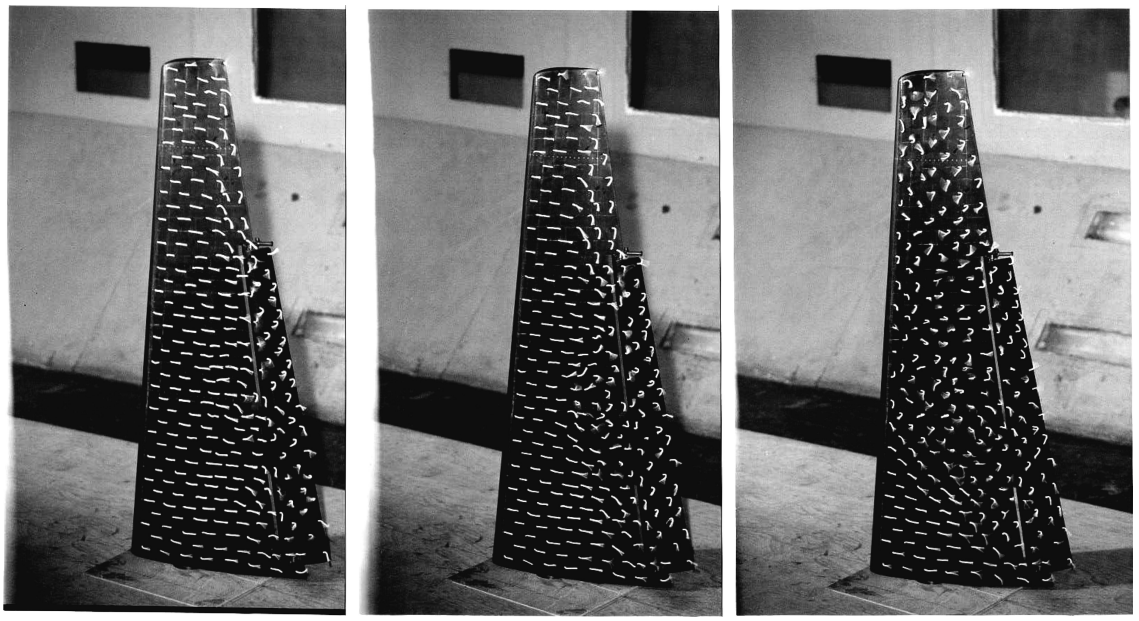

a) $\alpha = 6$ deg b) $\alpha = 12$ deg c) $\alpha = 18$ deg

Fig. 8 Wing flow patterns using tufts at $\delta_f = 30$ deg.

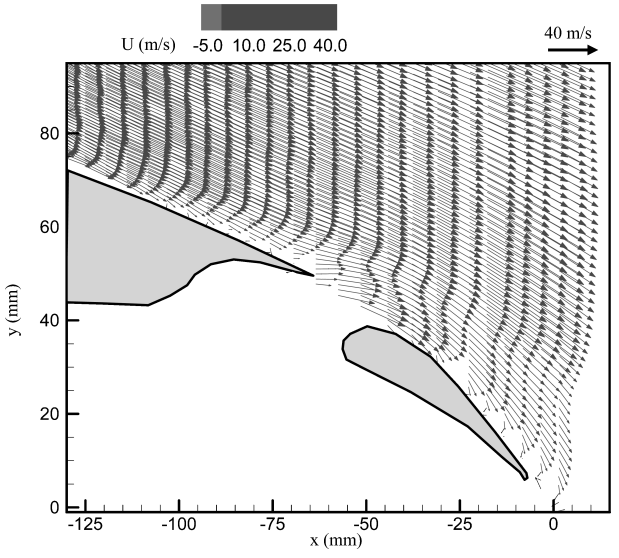

Fig. 9 Mean velocity field at $\alpha = 10.5$ deg for flap deflection of 20 deg.

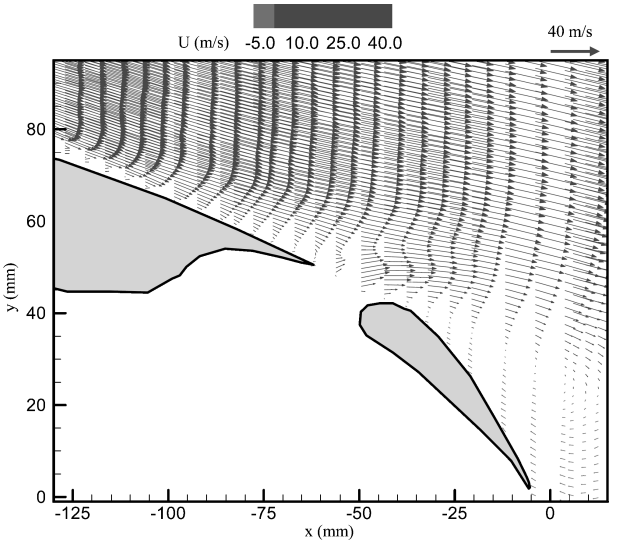

Fig. 11 Mean velocity field at = 10.5 deg for flap deflection of 30 deg.

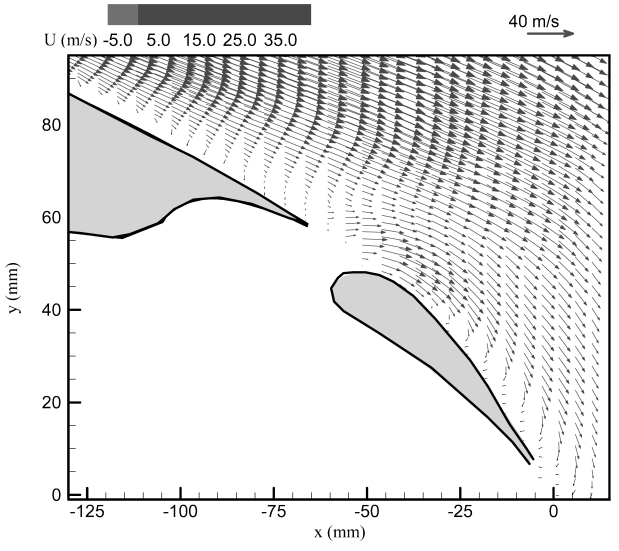

Fig. 10 Mean velocity field at $\alpha = 15.5$ deg for flap deflection of 20 deg.

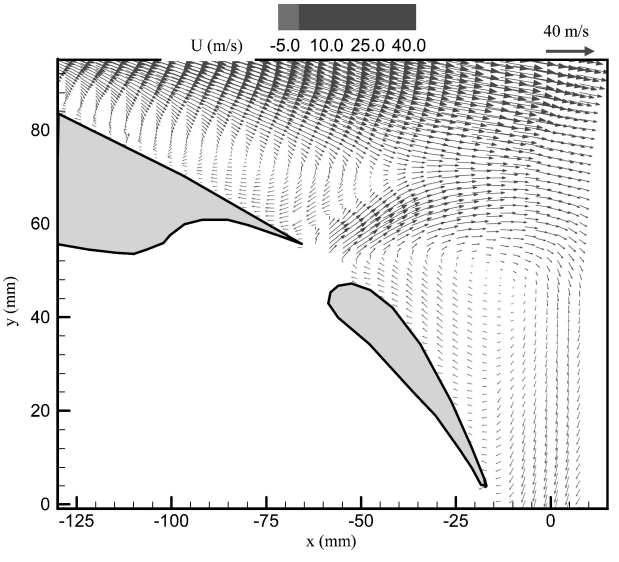

Fig. 12 Mean velocity field at $\alpha = 15.5$ deg for flap deflection of 30 deg.

$\alpha = 10.5$ deg, $\delta_f = 20$ deg, but the flow is significantly separated over a good part of the flap due to higher adverse pressure gradient. The slot flow locally is nearly parallel to the freestream direction and has relatively low magnitude. At $\alpha = 15.5$ deg, on the other hand, the slot flow is energetic and has a jetlike character, virtually bifurcating the flow on either side of it. A large-scale separation on the main wing ahead of the trailing edge and a massively separated flow over the flap may be observed. The maximum velocity in the slot flow jet was about 20 m/s that is, 50% of U_∞, and the maximum reversed flow velocities on the flap were about 3 and 5 m/s for $\alpha = 10.5$ and 15.5 deg, respectively. Thus, the PIV measurements have captured the complex flow topology including flow reversals quite well. It may also be inferred that the closure of the separated flow on the flap at $\alpha = 10.5$ and 15.5 deg will occur well downstream of the flap (which is not documented in this study).

The preceding results of the mean velocity field at the two flap deflections show certain major features of separated flow on the wing and flap and local features of flow through the slot. It is clear that the slot flow, its magnitude and direction, is strongly dependant on the wing incidence, flap position, and its deflection. The presence of separated flow, although varying in degree in the earlier documented cases, possibly results in the hysteresis in the aerodynamic loads. It is believed that the energetic jetlike slot flow at $\alpha = 15.5$ deg and $\delta_f = 30$ deg is responsible for the observation of double-loop hysteresis; with such massive separation ahead of trailing edge and on the flap, it is perhaps conceivable that the flow topology for the increasing and decreasing values of incidence, are not necessarily be the same (unlike attached flow on the wing and the flap), resulting in strong hysteresis.

It is clear that the flap position in relation to the main wing trailing edge will have significant influence on the slot flow. It has been suggested by Biber and Zumwalt[14] that the slot flow angle (Fig. 13) is an important parameter determining the level of hysteresis. (The slot flow angle β was defined as the angle between the slot flow vector and wing chord line; the slot flow vector was defined as the normal to the minimum radius line from the wing trailing edge to the flap leading edge.) This may be seen as a geometric definition of the slot flow vector. We have compared the values of β obtained using the preceding geometric definition with those inferred from the PIV mean velocity data (Figs. 9–12) in Table 1; the value of β from PIV may be seen to be some kind of a local average in the slot zone and, therefore, prone to larger errors of 2–3 deg.

Table 1 Comparison of slot flow vector angles

δ_f, deg	α, deg	Slot flow angle β (geometry), deg	Slot flow angle β(PIV), deg
	10.5	45	−3
20			
	15.5	46	15
	10.5	51	24
30			
	15.5	52	50

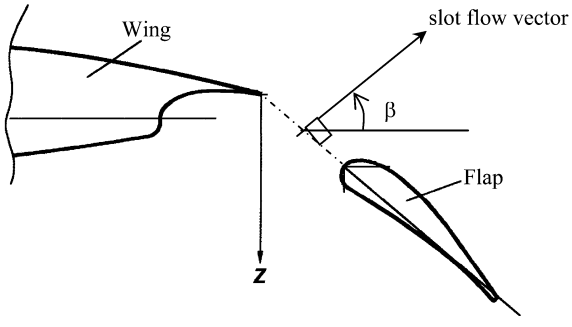

Fig. 13 Comparison of slot flow vector angles.

The actual slot flow angle is, in general, very different from the slot flow angle determined using the airfoil flap slot geometry except at $\alpha = 15.5$ deg and $\delta_f = 30$ deg, where the close agreement observed is a coincidence. These results strongly suggest that the slot flow angle is not determined by local geometry but by the overall flow on the wing and flap.

Conclusions

Experiments have been performed at low speeds documenting certain broad aspects of hysteresis on a mildly swept wing under high-lift conditions. Aerodynamic load measurements were carried out at two values of incidence of 10.5 and 15.5 deg and flap deflections of 20 and 30 deg, essentially under quasi-steady conditions (very similar to those on a GAW-2 airfoil[14]). Two-dimensional PIV was utilized to measure the mean velocity vector field in the rear part of the wing and flap.

Mild and massive double-loop hysteresis loops were observed for the flap deflections of 20 and 30 deg, respectively. The mean velocity field obtained by two-dimensional PIV for the four cases revealed certain complex features including significant zones of reversed flow. The occurrence of hysteresis is obviously a consequence of separated flows on the airfoil–flap combination at the higher incidence. It is suggested that the energetic jet-like slot flow observed at $\alpha = 15.5$ deg and $\delta_f = 30$ deg is a major feature associated with the massive double-loop hysteresis observed in the aerodynamic loads.

The slot flow angle determined from the PIV measurements is in general very different from those estimated using the airfoil–flap–slot geometry, suggesting that the slot flow angle is not determined by local geometry, but by the overall flow on the wing and flap. This could have certain strong implications in modeling high-lift flows by engineering methods, for example, viscous–inviscid interactive calculations.

Acknowledgments

The authors thank the Aeronautical Research and Development Board, Government of India, for funding this research. Sincere thanks are due to M. S. Kamaleshiah of Centre for Civil Aircraft Design and Development National Aerospace Laborrattories for his valuable support during the wind-tunnel tests at the Indian Institute of Science. The support of the staff of the 1.5-m low-speed wind tunnel in carrying out the particle image velocimetry experiments is gratefully acknowledged.

References

[1]Van Dam, C. P., "The Aerodynamic Design of Multi-Element High-Lift Systems for Transport Airplanes," *Progress in Aerospace Sciences*, Vol. 38, No. 2, Feb. 2002, pp. 101–144.

[2]Meredith, P. T., "Viscous Phenomena Affecting High-lift Systems and Suggestions for Future CFD Development," High-Lift System Aerodynamics, CP 515, AGARD, Paper 19, Sept. 1993.

[3]Van Dam, C. P., Los, S. M., Miley, S. J., Roback, V. E., Yip, L. P., Bertelrnd, A., and Vijgen, P. M. H. V., "In-Fight Boundary-Layer State Measurements on a High-Lift System: Main Element and Flap," *Journal of Aircraft*, Vol. 4, No. 6, 1997, pp. 757–763.

[4]Lin, J. C., Robinson, S. K., McGhee, R. J., and Valarezo, W. O., "Separation Control in High-Lift Airfoils via Micro-Vortex Generators," *Journal of Aircraft*, Vol. 31, No. 6, 1994, pp. 1317–1323.

[5]Brune, G. W., and Sikavi, D. A., "Experimental Investigation of the Confluent Boundary Layer of a Multielement Low Speed Airfoil," AIAA Paper 83-0566, Jan. 1983.

[6]Nakayama, A., Kreplin, H. P., and Morgan, H. L., "Experimental Investigation of Flowfield About a Multi-element Airfoil," *AIAA Journal*, Vol. 28, No. 1, 1990, pp. 14–21.

[7]Biber, K., and Zumwalt, G. W., "Flowfield Measurements of a Two-Element Airfoil with Large Separation," *AIAA Journal*, Vol. 31, No. 3, 1993, pp. 459–464.

[8]McGinley, C. B., Anders, J. B., and Spaid, F. W., "Measurements of Reynolds Stress Profiles on a High-Lift Airfoil," AIAA Paper 98-2620, June 1998.

[9]Ying, S. X., Spaid, F. W., McGinley, C. B., and Rumsey, C. L., "Investigation of Confluent Boundary Layers in High-Lift Flows," *Journal of Aircraft*, Vol. 36, No. 3, 1999, pp. 550–562.

[10]Seelhorst, K. A., Buetefisch, K. A., and Weiland, M., "3-Component LDV for Near-Wall Measurements on a Multi-Element High-Lift Airfoil Configuration," *16th ICIASF Congress*, 1995, pp. 167–173.

[11]Kuhn, W., Kompenhans, J., and Monnier, J. C., "Full Scale PIV Test in an Industrial Facility," *Particle Image Velocimetry*, edited by M. Stanislas, J. Kompenhans, and J. Westerweel, Kluwer Academic, Dordrecht, The Netherlands, 2000, pp. 91–150.

[12]Carmichael, B. H., "Low Reynolds Number Airfoil Survery," NASA CR 165803, Vol. 1, 1981, pp. 55–57.

[13]Mueller, T. J., "Low Reynolds Number Vehicles," AGARD-AG-288, Feb. 1985.

[14]Biber, K., and Zumwalt, G. W., "Hysteresis Effects on Wind Tunnel Measurements of a Two-Element Airfoil," *AIAA Journal*, Vol. 31, No. 2, 1993, pp. 326–330.

[15]Landman, D., and Britcher, C. P., "Experimental Investigation of Multielement Airfoil Lift Hysteresis due to Flap Rigging," *Journal of Aircraft*, Vol. 38, No. 4, 2001, pp. 703–708.

[16]Krothapalli, A., Venkatakrishnan, L., Lourenco, L., and Elavarasan, R., "Turbulence and Noise Suppression of a High-Speed Jet by Water Injection," *Journal of Fluid Mechanics*, Vol. 491, 2003, pp. 131–159.